Non-invasive technique for assessment of vascular wall stiffness using laser Doppler vibrometry

Non-invasive technique for assessment of vascular wall stiffness using laser Doppler vibrometry

Adriaan Campo[1], **Patrick Segers**[2], **Hilde Heuten**[3], **Inge Goovaerts**[3], **Guy Ennekens**[3], **Christiaan Vrints**[3], **Roel Baets**[4] **and Joris Dirckx**[1]

[1] Laboratory of Biomedical Physics, Faculty of Science, University of Antwerp, Groenenborgerlaan 171 B-2020 Antwerp, Belgium
[2] bioMMeda, Institute Biomedical Technology, Ghent University, Blok B, De Pintelaan 185, B-9000 Gent, Belgium
[3] Departement of Cardiology, University Hospital Antwerp, Antwerp, Wilrijkstraat 10, 2650 Edegem, Belgium
[4] Photonics Research Group, Ghent University, Sint-Pietersnieuwstraat 41, 9000 Belgium

E-mail: adriaan.campo@ua.ac.be

Abstract

It has been shown that in cardiovascular risk management, stiffness of large arteries has a very good predictive value for cardiovascular disease and mortality. This parameter is best known when estimated from the pulse wave velocity (PWV) measured between the common carotid artery (CCA) in the neck and femoral artery in the groin, but may also be determined locally from short-distance measurements on a short vessel segment. In this work, we propose a novel, non-invasive, non-contact laser Doppler vibrometry (LDV) technique for evaluating PWV locally in an elastic vessel. First, the method was evaluated in a phantom setup using LDV and a reference method. Values correlated significantly between methods ($R \leqslant 0.973$ ($p \leqslant 0.01$)); and a Bland–Altman analysis indicated that the mean bias was reasonably small (mean bias $\leqslant -2.33$ ms). Additionally, PWV was measured locally on the skin surface of the CCA in 14 young healthy volunteers. As a preliminary validation, PWV measured on two locations along the same artery was compared. Local PWV was found to be between 3 and 20 m s^{-1}, which is in line with the literature (PWV = 5–13 m s^{-1}). PWV assessed on two different locations on the same artery correlated significantly ($R = 0.684$ ($p < 0.01$)). In summary, we conclude that this new non-contact method is a promising technique to measure local vascular stiffness in a fully non-invasive way, providing new opportunities for clinical diagnosing.

1. Introduction

There exists a well-known relationship between arterial stiffness and cardiovascular risk, and stiffness of large arteries has been shown to be a very robust predictor for cardiovascular morbidity and mortality [1, 2].

Increased arterial stiffness increases arterial impedance. As such, when the heart ejects a given stroke volume, this will be done at a higher arterial blood pressure [3]. In addition, increased arterial stiffness leads to increased velocity of the

pressure waves emerging from the heart, or an increased pulse wave velocity (PWV). This is illustrated in the classical Moens–Korteweg equation (1) giving the relation between the PWV, the elastic modulus (E), the thickness of the wall (h), the lumen diameter (D) and the density of the blood (ρ) in a thin walled tube ($h \ll D$) [4]:

$$\text{PWV} = \sqrt{Eh/(\rho D)}. \tag{1}$$

The waves reflecting in the periphery will, because of the higher PWV, return earlier to the heart, adding to the systolic
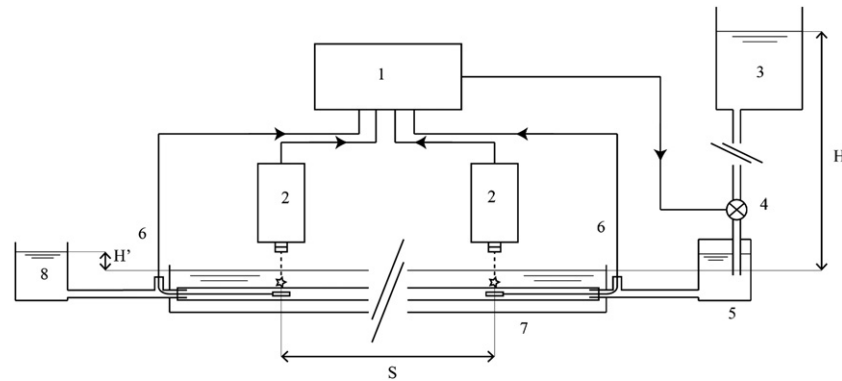
Figure 1. Diagram of the phantom setup. (1) Console for data acquisition and valve steering; (2) laser Doppler vibrometers; (3) inflow and water reservoir with constant water level at height *H* above the water level in the water tank; (4) remote controlled valve; (5) Windkessel chamber; (6) pressure sensors; (7) latex tube suspended in a tank filled with water; (8) outflow and water reservoir with constant water level at height *H′* above the water level in the water tank. Both vibrometers and pressure sensors assessed the latex tube a distance *S* apart.

pressure [5]. Eventually, these and other related mechanisms may lead to hypertrophy of the heart, alteration of myocardial perfusion and increased systolic dysfunction [6].

Reliable methods to estimate arterial stiffness therefore represent significant clinical interest. One way to assess arterial stiffness is by measuring the PWV.

In vivo, most PWV measurement techniques require knowledge about the distance between two measuring points and the time required for the pulse wave to travel between these points (pulse transit time, or PTT). PWV can be measured on a systemic scale or on a local scale. Systemic PWV is typically measured between the common carotid artery (CCA) in the neck, and the femoral artery (FA) in the groin, and therefore reflects the overall elastic properties of the large systemic arteries. An increased PWV measured with the latter method is a predictor of coronary heart disease [2] and stroke [2, 7]. However, PWV assessment in this way is a fairly crude measurement, prone to error [8–10]. As the wave travels along the whole arterial system, its shape is modified because of the differences in arterial wall properties along the trajectory. Therefore, the characteristic time-points of the pulse wave used to determine the PTT are shifted, and the estimation of the PTT becomes problematic [11]. The distance between the two measurement locations can be reliably estimated with a simple tape measure and a scaling factor. This, however, does not represent the actual distance traveled by the pulse, and distance measurements can become unreliable when patients with high BMI or high age are considered [12].

The large arteries are predominantly affected by arteriosclerosis and atherosclerosis as reflected in the PWV [13]. Moreover, increased PWV in the large arteries has a possible direct effect on cardiovascular health [13]. Therefore, it has been hypothesized that a method to assess the stiffening of these large arteries has significant diagnostic value as addition to or even replacement of carotid-femoral PWV; and methods to measure PWV and dynamics of the vascular wall in a non-contact, non-invasive manner on a local scale attract a lot of interest [14]. Most local PWV measurement techniques focus on the CCA, surfacing in the neck, due to the fact that it is a large elastic artery with properties that may be representative for the aorta, and it is a key vessel providing blood flow to

the brain, often involved in the pathophysiology of stroke. Several non-invasive methods have been developed that allow measurement of the PWV locally in a vessel. Some of these methods have been tested both in a phantom and *in vivo* [15–17], others are invasive [18] or were only tested in phantoms [19, 20]. However, all of these methods require contact with the patient; they require trained personnel to handle echography equipment or clinical staff to perform invasive actions safely.

In this study, we propose an approach based on the use of laser Doppler vibrometry (LDV) [21, 22] providing a non-contact, non-invasive method to asses PWV locally in an elastic vessel. The motion of the vessel wall is in direct relation to the pressure inside the vessel. By assessing wall velocity with LDV, it is possible to detect the pulse wave at two locations along the trajectory of the vessel and to calculate the PWV. And from the PWV, the stiffness of the vessel wall can be determined. Previous experiments indicate that LDV can be used to measure carotid-femoral PWV [23]. In this study, we assess the feasibility of the method to measure local PWV, hereby making use of a phantom setup and a small group of young healthy volunteers.

2. Materials and methods

2.1. LDV for PWV detection

LDV measures the velocity of a moving object using interference of light. A low power laser beam (<1 mW) is aimed at the object. When the object moves, the frequency of the reflected light is shifted due to the Doppler effect. LDV uses this reflected light to generate an electrical output signal which is directly proportional to the velocity of the moving object [21, 22]. In the current method, the beam is directed at the outside wall of a tube or at the skin above a superficial artery.

2.2. Phantom experiment

2.2.1. Experimental setup. To evaluate the precision and the accuracy of LDV for measurement of PWV *in vivo*, a phantom setup mimicking arterial pulse propagation was built (see figure 1).

Looking downstream, this setup consists of a water reservoir with constant water level H, a remote controlled valve, a partly filled vessel acting as Windkessel, a test tube suspended in a water tank with constant water level h 30 cm below H, another water reservoir with constant water H' slightly above h and finally the outflow. Constant water levels were maintained by using pump and overflow mechanism. At both sides of the test tube, a small pressure sensor mounted on the end of a thin wire (Micro-cath and PCU-2000, Millar Instruments, Houston, USA) entered the test tube by use of T-connectors, allowing the assessment of pressure inside the tube. Two vibrometers (OFV-534 and OFV-5000, Polytec, Waldbronn, Germany) were aimed downwards on the wall of the test tube at the location of the pressure sensors, allowing assessment of the radial velocity of the tube wall. Small pieces of reflective tape were used to enhance the vibrometer signal.

In order to simulate the propagation of a pulse in an artery, the valve was opened briefly, resulting in a square pressure wave in the system with amplitude related to H. H was chosen as 30 cm, approximating the amplitude of the arterial pressure wave in the CCA. The Windkessel effect rounded the resulting pressure wave before entering the test tube. The test tube was suspended in water to achieve homogeneous radial expansion at internal pressure increase, and to damp unwanted vibrations. H' was chosen slightly higher than h, so the lumen of the test tube would remain open at all times.

2.2.2. PWV measurements.

In consecutive experiments, three types of thin walled latex test tubes were mounted in the water tank. The latex tubes respectively had length of 46 cm and inner diameter of 15 ± 1 mm (type 1; Kendall, Argyle, Tullamore Ireland); length of 30 cm and inner diameter of 8 ± 1 mm (type 2; Kendall); and length of 80 cm and inner diameter of 6 ± 1 mm (type 3; Silkolatex, Rüsch, Weiblingen, Germany) according to measurements with a tape measure; and respective wall thickness of 0.36 ± 0.01 (type 1); 0.32 ± 0.01 (type 2); and 0.13 ± 0.01 mm (type 3) according to measurements with a digital caliper. These tubes were chosen because the sizes of their lumen and presumed PWV are of the same order of magnitude as those of the largest blood vessels. During a single measurement, both the velocity of the tube wall displacement and the pressure inside the tube were assessed with the vibrometers and the pressure sensors, respectively. A single measurement consisted of six cycles. Each cycle, the valve was opened for 100 ms followed by 9.9 s of rest in order to allow any reflections and vibrations to damp out, i.e. a cycle takes 10 s, and one measurement takes 60 s. For further processing, only data from the five last cycles were used, as the first cycle was considered a 'dummy'. For every cycle of every measurement, the data were used to calculate PTT as described below.

The positions of the sensors were chosen a certain distance S apart, as determined with a tape measure. Measurements were repeated for six different distances S ($S = 2.5, 5, 10, 15, 20$ and 25 cm for tube types 1 and 3; $S = 2.5, 5, 7.5, 10, 15$ and 20 cm for tube type 2). Each time, one measurement location was kept fixed while the other measurement location was positioned 2.5–25 cm downstream of the former. For each distance, measurements were repeated three times. This experiment as a whole was repeated three times for each tube. The output from the vibrometers and the pressure sensors was sampled with a data acquisition card (NI-DAqx, National Instruments, Austin, USA) at 50 000 samples per second.

2.2.3. Data analysis.

In order to validate the results, three different established algorithms were used to calculate the PTT for every cycle from every measurement (see figure 2).

In the first algorithm, the delay between the maxima of the second-order differentiated signal of the pressure sensors, or the first-order differentiated signal from the vibrometers, was used to assess the PTT and is further referred to as the 'second derivative method' (SDM) [11].

In the second algorithm, the intersections between the horizontal line going through the 'foot' of the pressure signal or the integration of the vibrometer signal, and the tangent of the same signal, was used to assess the PTT. The position and the slope of the tangent are determined through the first-order differentiated signal from the pressure sensors, or the vibrometer signal. The latter method is further referred to as the 'tangent-intersect method' (TIM) [11].

In a third approach, the PTT was calculated by cross-correlating the vibrometer signal, or the first-order differentiated signal of the pressure sensors from two measurement spots. Cross-correlation is a measure of similarity of two waveforms as a function of a time-lag applied to one of them. For two discrete functions f and g, and a time-lag k, the normalized cross-correlation function r_{fg} is defined as

$$r_{fg}(k) = \frac{1}{n-k} \frac{\sum_{t=1}^{n-k} (f(t) - \mu_f)(g(t+k) - \mu_g)}{\sigma_f \sigma_g}, \quad (2)$$
$$k = -n+1, \ldots, n-1$$

with μ_f and μ_g being the mean, and σ_f and σ_g being the standard deviations of the respective waveforms. Time-lag k is modulated until an optimal correlation is reached. In order to avoid the effect of reflections, only the first ascending part of the pressure signal and the integration of the vibrometer signal are used in this analysis. This method is further referred to as the 'cross-correlation method' (XCM) [24].

Before the application of the described algorithms, data were filtered using a fourth-order low pass Butterworth filter using Matlab with cutoff frequency of 40 Hz and a second-order high pass Butterworth filter with cutoff frequency of 0.05 Hz in order to remove spurious effects from the measurement environment. A high pass filter was introduced in order to filter slow movements due to fluid flow in the tube and the water tanks. The cutoff frequency was set well below the pulse frequency. A low pass filter was used to remove noise and spikes.

The cutoff frequency for the low pass filter was set at 40 Hz, about 20 Hz below the frequency of small ripples in some of the datasets, originating from the noisy lab environment. The overall shape and detail of the waveforms were not altered visibly by the filtering step.

Five PTT values from three repetitions of three measurements were used to calculate an average and a standard
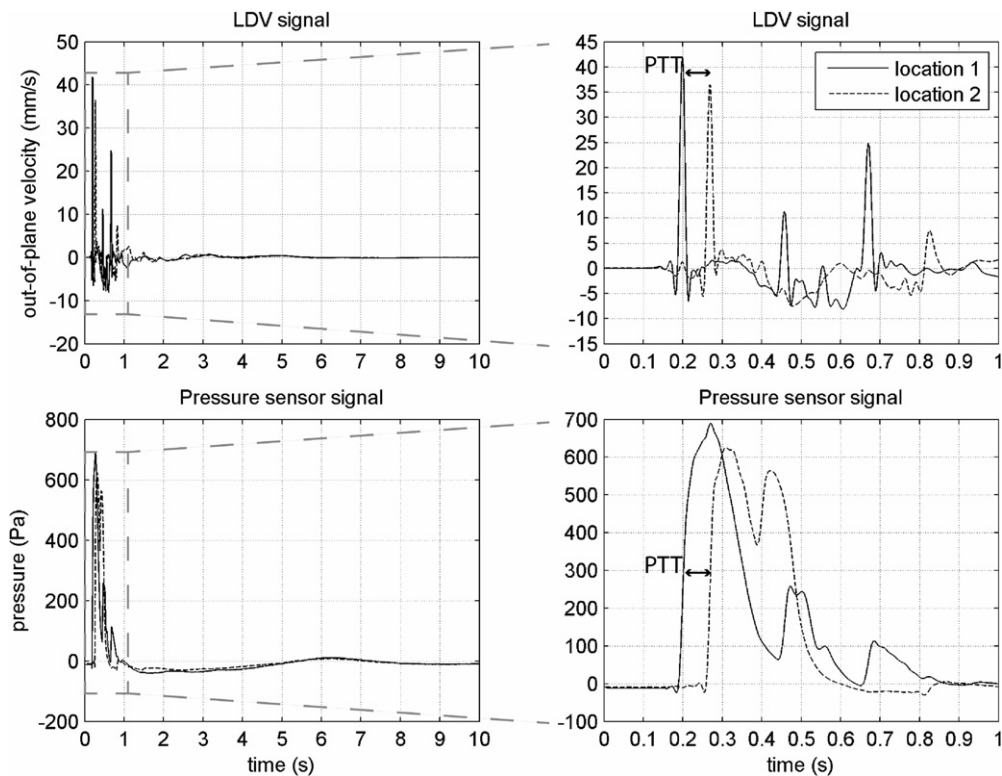
Figure 2. LDV signal obtained on the tube wall and pressure sensor signal measured in tube type 1 during one cycle at the two different measurement locations (location 1 and location 2). The time needed for the pressure wave to travel between two locations or the pulse transit time (PTT) was calculated with several different algorithms, as indicated with arrows in the right panels. The low pass cutoff of the filter is set at 40 Hz.

deviation for every distance between measurement spots ($N = 54$ for every distance S). Measurement error on the distance measurements was determined as the smallest scale unit on the tape measure, and PWV was calculated simply as

$$\text{PWV} = \frac{S}{\text{PTT}}. \qquad (3)$$

Subsequently, measurement error for PWV was calculated from the standard deviation on PTT and the measurement error on S. Additionally, PTT values with the LDV and the pressure sensor method were subjected to a Spearman's correlation analysis (SPSS Statistics 20, IBM, Armonk, USA), and a Bland–Altman assessment for agreement.

2.3. In vivo experiment

2.3.1. Experimental setup. In a feasibility study of the method *in vivo*, arterial PWV of the CCA was assessed in human test subjects. The subject was asked to lie down on a stretcher. The position of the right CCA was found by carefully palpating the region in the neck. Eventually, three reflective patches were applied on the skin in a straight line along the trajectory of the CCA, depending on the shape and anatomy of the neck region. Patches were applied about 1 cm apart depending on the length of the accessible region. Eventually, two LDV systems were aimed and focused on two reflective patches.

When an arterial pressure pulse propagates through the artery, the artery will distend, causing radial displacement of the arterial wall. The LDV measures the velocity of this radial

wall displacement at one discrete spot. By using two LDV's aimed at two spots on the artery some short distance apart, two velocity signals are obtained, which are nearly identical, but which are shifted in time due to the delay between the passing of the pressure pulse along the two spots. By measuring the time shift between the two velocity signals, the propagation velocity of the pulse can be readily obtained. Because the shape of the pressure pulse slightly changes along the length of the tube, the two subsequent velocity signals are not fully identical and a good method is needed to calculate the time shift (see section 2.2.3).

At the measurement site, the CCA lies just below the surface, such that CCA distension causes displacement of the skin. An LDV system aimed perpendicularly to the skin, right on top of the artery, will detect the velocity of the out-of-plane displacement of the skin. Measured velocities in this manner are around 10 mm s^{-1}, which is in line with findings from US techniques measuring the displacement of the arterial wall [20]. Since the LDV signal is proportional to velocity [21, 22], it is nearly insensitive to background motions. This is very important in future clinical applications: at the level of the artery, several other out-of-plane velocity components are present. Velocities from breathing, for example (as measured on the jaw), are on average less than 3 mm s^{-1}. Velocities from slow muscle movements, or drift in the setup, are even lower. Swallowing, however, is a major disturbing factor, and renders a measurement unusable.

Measurements can be performed on bare skin, but then much less light is reflected, deteriorating the quality of the

4
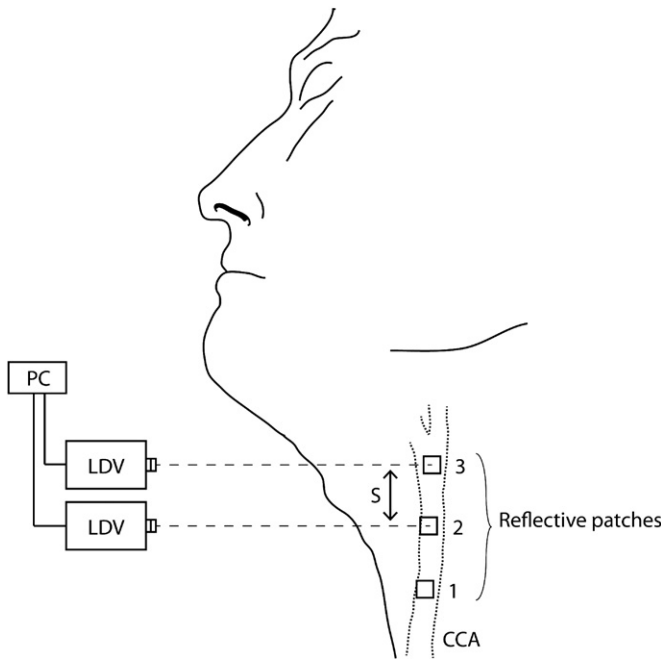
Figure 3. Arterial PWV was assessed in 16 young healthy test subjects aged between 20 and 30 (5 female and 11 male). The position of the right CCA (CCA, dotted line) was found by carefully palpating the region in the neck. Three reflective patches (reflective patches 1–3) were applied on the skin in a straight line along the trajectory of the CCA. Patches were put a certain distance (*S*) apart as determined with a tape measure. Two vibrometers (LDV) were aimed and focused on two reflective patches at a time. Output was send to an acquisition card at 125 000 samples per second (PC).Measurements were repeated 4–7 times comparing two different measurement locations: one more upstream (on reflective patches 1 and 2) and one more downstream (on reflective patches 2 and 3) of the considered segment.

signal. Application of pieces of reflective tape or reflective make-up greatly enhances the signal [23], but of course it involves touching the subject. In this sense, the method as a whole is not non-contact. We use the term non-contact to emphasize that during the measurement itself there is no mechanical hampering of the blood vessels, leaving their mechanical properties fully unaltered.

2.3.2. PWV measurements. PWV measurements were performed in 16 young healthy test subjects aged between 20 and 30 (5 female and 11 male). Just prior to a measurement, the test subject was asked to hold as still as possible, to hold his breath, and to avoid swallowing during the measurement. Beginning and ending of the measurement were indicated with audible cues. A measurement lasted 20 s. The output from the vibrometers was sampled with a data acquisition card (NI-DAqx, National Instruments, Austin, USA) at 125 000 samples per second. Measurements were repeated 4–7 times comparing two different measurement spots: one upstream (on patches 1 and 2) and one more downstream (on patches 2 and 3) of the considered segment (see figure 3). The distance *S* between measurement spots was determined with a tape measure, and was always between 1 and 2 cm as measured between two consecutive measurement spots.

2.3.3. Data analysis. Due to the complexity of the *in vivo* LDV signal in this instance, the whole signal from two measurement spots was compared with cross-correlation (as described in section 2.2.3), in order to obtain the PTT (see figure 4). This was done without further processing, as a filtering step did not alter the result considerably, also reported by Hermeling [11]. However, when necessary, a simple high pass filter can remove most slow velocity components, since they have a much lower frequency than the frequency of interest (heartbeats). PWV was further calculated as in (3) for every measurement. Eventually, an average PWV with standard deviation was calculated. Complete datasets of two male participants were discarded due to unwanted artifacts discovered *a posteriori* (sets contained too much unwanted body movement causing saturation of the LDV signal, rendering further processing impossible). Additionally, upstream and downstream PWV values were subjected to a Spearman's correlation analysis (SPSS Statistics 20, IBM, Armonk, USA).

3. Results

3.1. Phantom measurements

As can be seen from figure 5, PWV is not consistent for different measurement locations: there is a drift in the registered PWV with PWV generally being lower upstream than it is downstream.

A Spearman's correlation analysis of both measuring approaches indicates a significant correlation between LDV and pressure sensors for the three algorithms: $R = 0.968$ ($p < 0.01$) for SDM, $R = 0.973$ ($p < 0.01$) for TIM and $R = 0.964$ ($p < 0.01$) for XCM (see figure 6).

The Bland–Altman analysis indicates that the 95% limits of agreement between the LDV method and the pressure sensor method to define the PTT ranged from -13.05 to 8.39 ms with a mean bias of -2.33 ms for SDM; from -11.73 to 7.63 ms with a mean bias of -2.05 ms for TIM; and from -12.11 to 8.71 ms with a mean bias of -1.70 ms for XCM (see figure 6).

In order to visualize the effect of the propagating pulse wave, data from different measurement positions can be plotted in a spatiotemporal diagram representing time and position along the tube versus the wall velocity and pressure, respectively (with time on one axis, measurement position on the other, and wall velocity or pressure linked to a gray color scale). Data depicted this way allow observation of the propagation of the pulse wave (see figure 7).

3.2. In vivo measurements

PWV values lay between 3 and 20 m s^{-1} for the human test subjects. Measured velocities have a large standard deviation in some female subjects (coefficient of variation (CV) > 30%). Measurements upstream and downstream are positively correlated according to a Spearman's correlation with $R = 0.684$ ($p < 0.01$) (see figure 8).
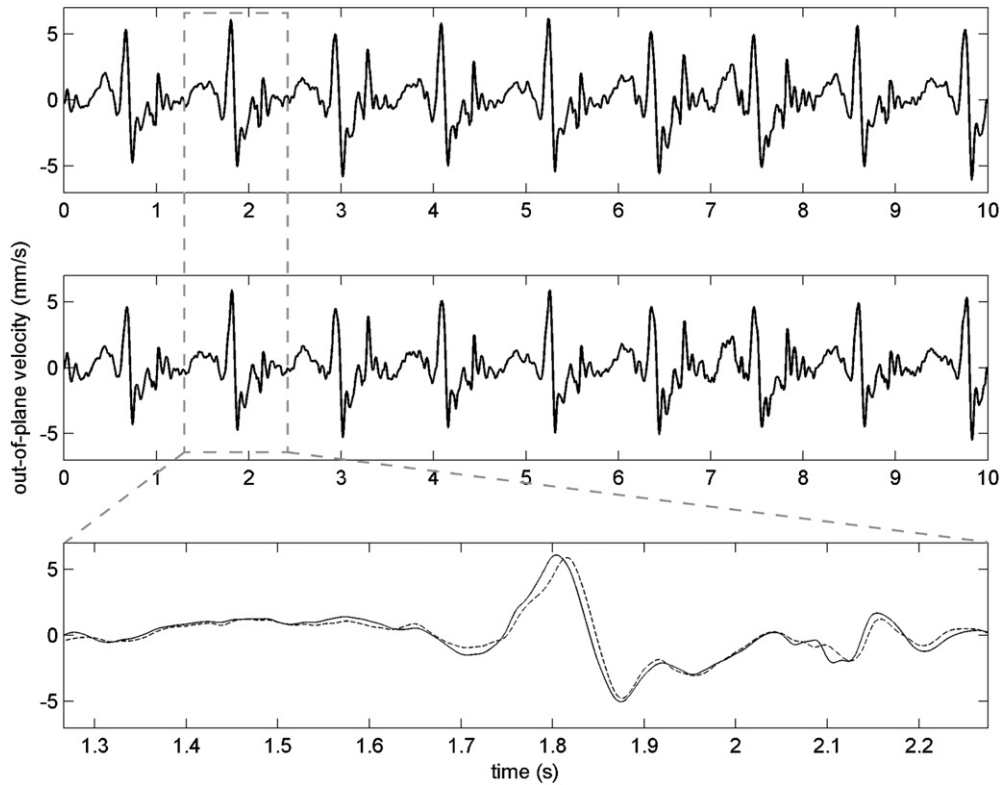
Figure 4. *In vivo* measurement of out-of-plane velocity of the skin at the level of the CCA. Depicted measurement was performed simultaneously at two measurement locations a distance of 1.5 cm apart. The upper panel was recorded more toward the chest; the middle panel was recorded more toward the chin (upstream relative to the former). The lower panel shows a detail from the upper two panels. The full line is a detail from the upper panel, the dashed line is a detail from the middle panel. The time lapse (PTT) between the two waves is visible. For calculation of the PTT, measurements of out-of-plane velocity at two sites along the CCA are cross-correlated.
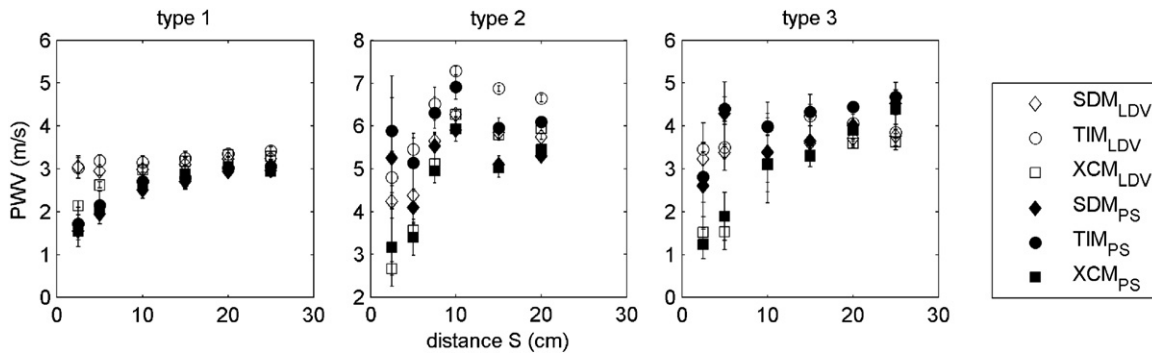

Figure 5. PWV data of the three different tube types, with the LDV and the pressure sensor measurement methods, using three different algorithms to calculate PTT. PTT values from five cycles from three repetitions of three measurements ($N = 54$) were used to calculate an average PTT value with standard deviation. Together with the measurement error on the distance measurement, an average PWV value and a PWV measurement error were calculated for six different distances S between measurement locations as depicted in the graphs.

4. Discussion and conclusion

Several approaches are possible for the determination of local PWV in the CCA. Methods for local PWV detection can be contact or non-contact. However, contact methods could introduce artifacts due to altering mechanical characteristics of the system, and they typically are less suited for large scale screening purposes. When aiming at a non-contact method for the determination of local PWV in the CCA, determination of PTT is needed, requiring at least two measuring points. The accessible portion of the human CCA is only a few centimeters

long, demanding a certain spatial and temporal resolution of the measurement technique. Therefore, LDV is suspected to be a suitable approach for local PWV detection. In LDV, the measuring points can be placed sufficiently close together, assessing surface motion with high temporal resolution.

The use of LDV was already explored to measure carotid-femoral PWV by De Melis *et al* [23]. However, here it is further developed to asses PWV locally in a large elastic artery such as the CCA *in vivo*. First, PWV was assessed with LDV as compared to a reference method in a phantom setup. Finally,
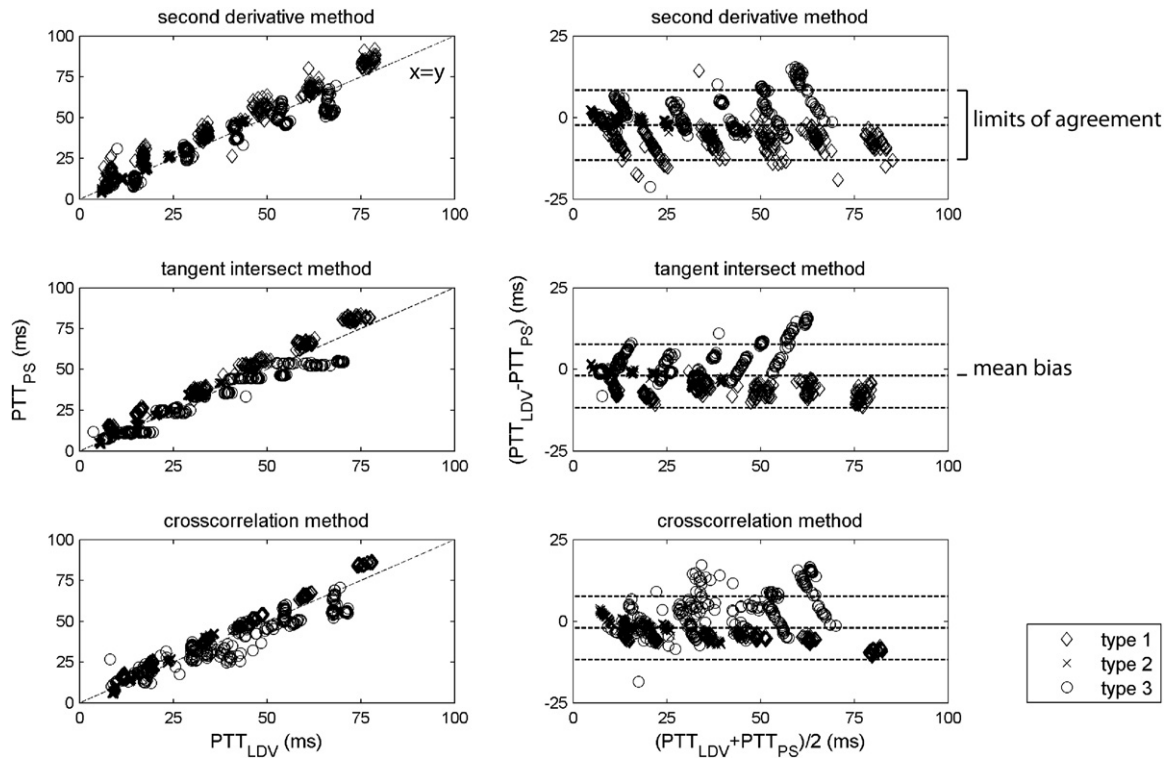
Figure 6. A Spearmans's correlation analysis (left panel) and a Bland–Altman assessment (right panel) were used to compare the LDV and the pressure sensor (PS) method to define the PTT. In the left panel, PTT as measured with LDV is on the horizontal axis (in ms) and PTT as measured with PS is on the vertical axis (in ms). A Spearman's correlation analysis of both measuring approaches indicates a significant correlation between LDV and pressure sensors for the three algorithms: $R = 0.968$ ($p < 0.01$) for SDM, $R = 0.973$ ($p < 0.01$) for TIM and $R = 0.964$ ($p < 0.01$) for XCM. In the right panel, $((PTT_{LDV} + PTT_{PS})/2$ is on the horizontal axis (in ms) and $(PTT_{LDV} - PTT_{PS})$ is on the vertical axis (in ms). The mean bias was defined as the mean of $(PTT_{LDV} - PTT_{PS})$. A range of agreement was defined as the mean bias $\pm 1.96 \times$ the standard deviation of the bias. The Bland–Altman analysis indicates that the 95% limits of agreement between the LDV method and the pressure sensor method to define the PTT ranged from -13.05 to 8.39 ms with a mean bias of -2.33 ms for SDM; from -11.73 to 7.63 ms with a mean bias of -2.05 ms for TIM; and from -12.11 to 8.71 ms with a mean bias of -1.70 ms for XCM.

LDV was used to assess PWV locally in the CCA in a small group of volunteers.

To illustrate the propagation of the pulse wave in the phantom setup, results of the two measurement methods were plotted in a spatiotemporal diagram representing time and position along the tube versus wall velocity and pressure, respectively (see figure 7). The propagation velocity in tube type 2 is higher, and the internal pressures are also higher. At the boundaries of the figure, wave reflections appear (see figure 7).

However, ideally PTT is determined using dedicated algorithms. Several algorithms are in use, even in commercial applications. Therefore, three different algorithms were evaluated in the phantom study: SDM, XCM and TIM.

For the three different algorithms, PTT values from LDV setup and pressure sensors are concurrent, as assessed with a correlation analysis and a Bland–Altman assessment for agreement.

Correlation analysis indicated that correlation coefficients are significant and close to 1 for the three algorithms, but best for SDM (see figure 6).

The Bland–Altman assessment of agreement indicated that both limits of agreement and mean bias are in the same range for the three algorithms, but the limits of agreement are

the narrowest for SDM and the mean bias is the closest to zero for XCM (see figure 6).

Although the outcomes are very much alike for the three algorithms, it is not possible to pick a preferred algorithm. SDM requires the least computational power, but it is more susceptible to noise, while XCM requires most computational power, and is susceptible to the effect of wave reflections [11].

However, measured PWV values are not consistent for different measurement locations (see figure 5). In all three tube types, and for all measurement approaches, a certain drift appears in measured PWV values. When measurement locations are taken further apart, measured PWV tends to become stable and very much comparable for all methods applied. Several explanations are possible for this phenomenon. As a measurement setup is seldom ideal, an array of artifacts may be present. For example, reflections of waves are obvious (see figures 2 and 7). Also, there is a gradual change in form and amplitude of the traveling pressure wave impeding comparison of the waveforms (see figure 2). Even more importantly, the suspended tube is able to move freely in all directions, performing other movements than just radial expansion. Movements of the tube in turn cause turmoil of the water in the water tank causing secondary movements. This drift in PWV values is also reported in other PWV studies (e.g. Chang *et al* [25]).
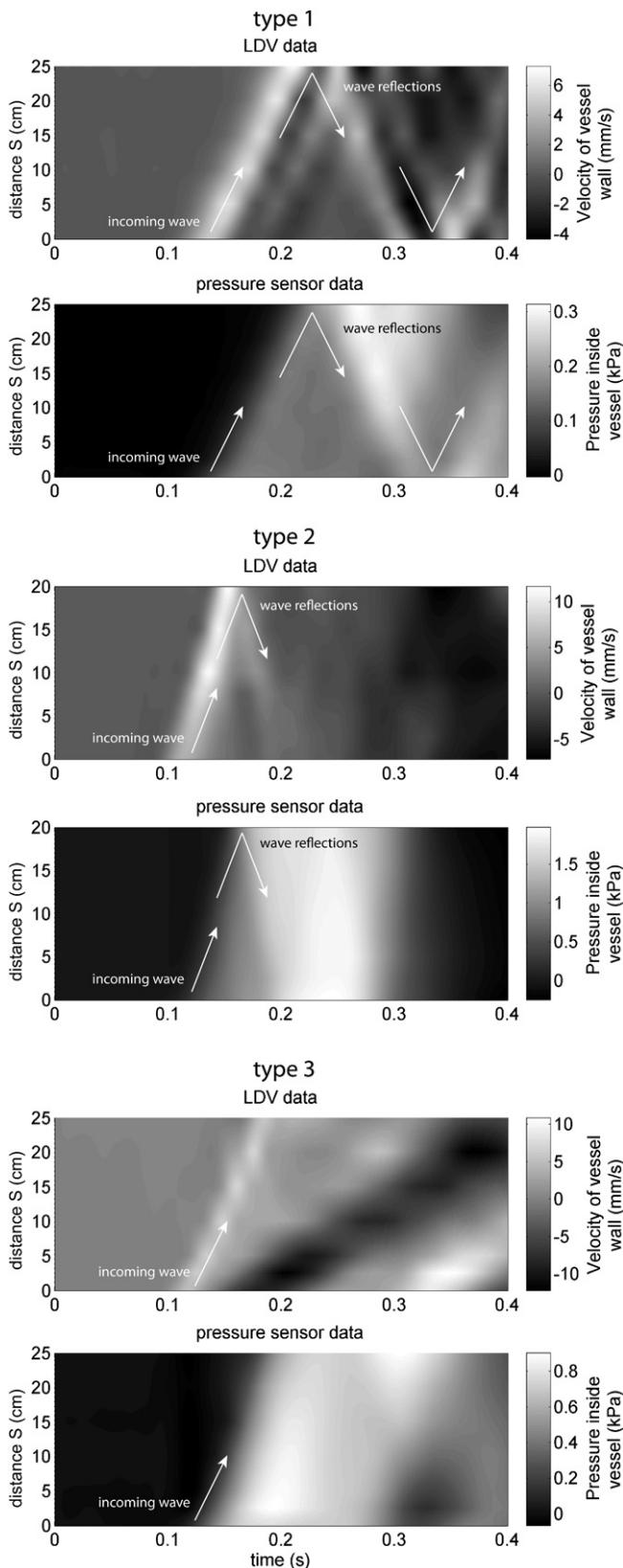
Figure 7. A spatiotemporal diagram representing time and position along the tube versus wall velocity and pressure respectively, using the *mesh* plot in Matlab (with time on one axis, measurement position on the other, and wall velocity or pressure linked to a gray color scale), showing the propagation of the pulse wave in the three tube types. PWV and internal pressure are in type 2. Wave reflections can be observed in type 1 and type 2 (white arrows).

In conclusion, the results of the phantom experiment prove that LDV is a feasible method to measure PWV in a laboratory context, on a local scale. However, artifacts due to imperfections in the measurement setup need to be considered, and are hard to rule out. The PWV values measured in the latex tubes are in the same range as those found in the large human arteries as well as the sizes of their lumen and the radial velocity of the tube wall, showing that these tubes are a good choice as a phantom material [4]. Data resulting from the measurements in the phantom setup encouraged us to perform a pilot study on a small group of volunteers.

However, when applied in an *in vivo* setting, this approach does pose specific challenges. First of all, using LDV, signals are measured unconstrained in any way, i.e. all tissues are allowed to move freely in all directions. Together with the high sample rate and time resolution of the method, this reveals the waveforms to be very complex and detailed, and a clear foot (as present in tonometry data) is often very hard to discern even for the trained eye. Also, a good reference method to measure PWV measurements is lacking, making it particularly hard to validate data acquired *in vivo*. We will discuss these issues below.

Different foot-finding algorithms have been described [11, 26]. These algorithms are known to give different results both *in vivo* and in phantoms, and currently there is neither a golden standard nor a consensus concerning foot-finding in arterial waveforms: approaches differ dramatically amongst authors, and even amongst commercial devices. In preparatory studies, several foot-finding algorithms for the detection of PTT *in vivo* were evaluated. These algorithms require careful preparation of the data. Also, they depart from specific characteristics of the shape of the waveform. Due to the nature of the LDV data, and due to the *in vivo* environment, several processing steps are needed before foot-finding algorithms can be applied, such as integration, differentiation, filtering and smoothing. All these steps change the shape of the waveform, and these steps become critical when very small PTT needs to be detected. The precarious task of finding the foot of a waveform therefore becomes even more challenging than is the case with other techniques, and attempts to develop a robust foot-finding algorithm for the detection of local PWV in the CCA *in vivo* were unsuccessful.

Cross-correlation on the other hand has the advantage that it requires no pre-processing of the data, and it circumvents the problem of foot-detection in complicated waveforms. The method has been used extensively in similar research [11, 17, 23, 24], and it performed well in the phantom setup.

A disadvantage of cross-correlation certainly is that this technique takes into account a larger portion of the waveform, increasing the effect of wave reflections on the detected PTT value. However, wave reflections and other artifacts are inherently linked to the non-ideal circumstances of an *in vivo* situation [14]. Because of the short length of the surfacing CCA segment, and the early appearance of a reflection point in the bifurcation, wave reflections will be present at a very early stage of the waveform, inevitably influencing foot-finding algorithms as well.

Based on the above arguments, it was concluded that cross-correlation is the method of choice here as a means to
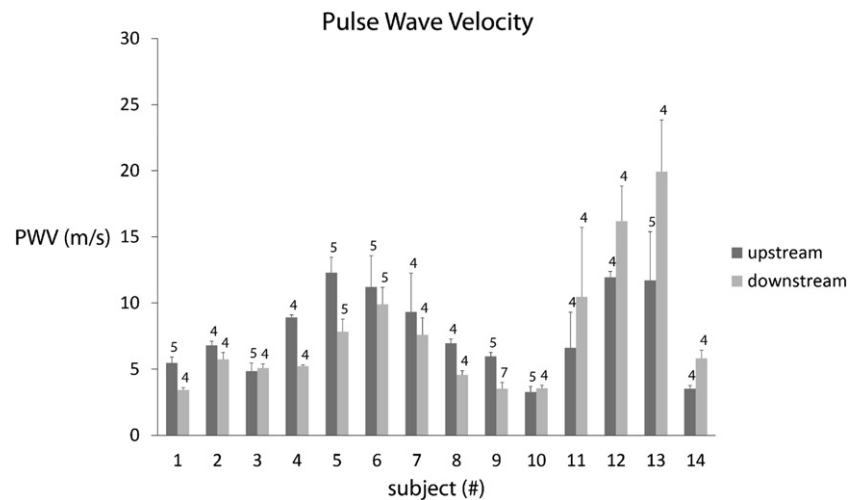
Figure 8. PWV values were acquired at two locations on the CCA. Bars represent average PWV and error bars represent matching standard deviation. Above each column, number of measurements *N* is indicated ($N = 4$–7). Results from the upstream location are depicted in dark gray; results from the downstream location are depicted in light gray. Subjects 1–9 are male and subjects 10–14 are female.

measure PTT in a local PWV measurement *in vivo*. This does of course not compromise the value of foot-finding algorithms in less localized applications.

Using cross-correlation, all *in vivo* PWV values were found to lie between 3 and 20 m s^{-1}, which is in the same order as literature values (between 5 and 13 m s^{-1} [4]).

As a preliminary validation, PWV measurements were executed at two different locations along the same arterial segment, hypothesizing that PWV values will be similar. It was found that PWV results at two measurement locations on the CCA are positively and significantly correlated. However, in some subjects, PWV values are not consistent for different measurement locations (see figure 8), as reflected in the Spearman's coefficient ($R = 0.684$ ($p < 0.01$)). This is possibly related to artifacts very similar to those seen in the phantom setup [25]: changing mechanical parameters along the CCA can cause a variation of PWV. The effects of damping and reflections can produce differences in waveforms (and hence influence PTT calculations). Additionally, standard deviations are markedly poorer in some measurements. This could be due to the fact that the carotid artery is smaller or more difficult to palpate in some subjects, making it harder to aim the LDV systems correctly (e.g. in females differences in carotid anatomy have been documented (e.g. Schulz *et al* [27]).

A good method for (local) PWV measurements is much sought after, and most or all available methods with potential for measuring PWV locally are still in an (early) stage of development. Therefore, results of the *in vivo* measurements could not be soundly validated with a state-of-the art reference method. However, comparison of the technique with pulse wave imaging (PWI) belongs to the future prospects.

In conclusion, we propose that by testing the LDV method on a phantom setup, and by comparing PWV values on the same arterial segment, a preliminary level of validation is provided, although further testing is needed with more test subjects, a reference method such as PWI, comparison between left and right CCA and an additional algorithm for detection of PTT (e.g. capable of detecting the dicrotic notch). Moreover,

it is suspected that posture during the measurement could have an influence on pulse wave behavior in the CCA, as indicated, for example, by Geinas *et al* [28], which should be taken into account for further development of this technique.

In summary, we put that this new non-contact method has potential to measure vascular stiffness in a fully non-invasive way. As preliminary results in phantoms and *in vivo* are promising, the method can be expected to provide new opportunities for clinical diagnosing. In future work, remaining issues concerning validation and detection of PTT will be tackled.

Acknowledgment

References

[1] Laurent S, Boutouyrie P, Asmar R, Gautier I, Laloux B, Guize L, Ducimetiere P and Benetos A 2001 Aortic stiffness is an independent predictor of all-cause and cardiovascular mortality in hypertensive patients *Hypertension* **37** 1236–41

[2] Mattace-Raso F U S *et al* 2006 Arterial stiffness and risk of coronary heart disease and stroke: the Rotterdam study *Circulation* **113** 657–63

[3] Chirinos J A, Segers P, De Buyzere M L, Kronmal R A, Raja M W, De Bacquer D, Claessens T, Gillebert T C, St John-Sutton M and Rietzschel E R 2010 Left ventricular mass: allometric scaling, normative values, effect of obesity, and prognostic performance *Hypertension* **56** 91–98

[4] Milnor W R 1982 *Hemodynamics* (Baltimore, MD: Williams and Wilkins)

[5] Schiffrin E L 2004 Vascular stiffening and arterial compliance. Implications for systolic blood pressure *Am. J. Hypertens.* **17** 39S–48S

[6] Boutouyrie P, Laurent S, Girerd X, Benetos A, Lacolley P, Abergel E and Safar M 1995 Common carotid artery stiffness and patterns of left ventricular hypertrophy in hypertensive patients *Hypertension* **25** 651–9

[7] Laurent S, Katsahian S, Fassot C, Tropeano A-I, Gautier I, Laloux B and Boutouyrie P 2003 Aortic stiffness is an independent predictor of fatal stroke in essential hypertension *Stroke* **34** 1203–6

[8] Van Bortel L M, Balkestein E J, van der Heijden-Spek J J, Vanmolkot F H, Staessen J A, Kragten J A, Vredeveld J W, Safar M E, Struijker Boudier H A and Hoeks A P 2001 Non-invasive assessment of local arterial pulse pressure: comparison of applanation tonometry and echo-tracking *J. Hypertens.* **19** 1037–44

[9] Millasseau S C, Stewart A D, Patel S J, Redwood S R and Chowienczyk P J 2005 Evaluation of carotid-femoral pulse wave velocity: influence of timing algorithm and heart rate *Hypertension* **45** 222–6

[10] Xu J 2003 Do we need a better approach for measuring pulse-wave velocity? *Ultrasound Med. Biol.* **29** 1373

[11] Hermeling E, Reesink K D, Reneman R S and Hoeks A P G 2007 Measurement of local pulse wave velocity: effects of signal processing on precision *Ultrasound Med. Biol.* **33** 774–81

[12] Huybrechts S A M, Devos D G, Vermeersch S J, Mahieu D, Achten E, de Backer T L M, Segers P and van Bortel L M 2011 Carotid to femoral pulse wave velocity: a comparison of real travelled aortic path lengths determined by MRI and superficial measurements *J. Hypertens.* **29** 1577–82

[13] McEniery C M, Wilkinson I B and Avolio A P 2007 Age, hypertension and arterial function *Clin. Exp. Pharmacol. Physiol.* **34** 665–71

[14] Hermeling E, Reesink K D, Hoeks A P G and Reneman R S 2010 Potentials and pitfalls of local PWV measurements *Am. J. Hypertens.* **23** 934 (author reply 935)

[15] Struijk P C, Wladimiroff J W, Hop W C J and Simonazzi E 1992 Pulse pressure assessment in the human fetal descending aorta *Ultrasound Med. Biol.* **18** 39–43

[16] Meinders J M, Brands P J, Willigers J M, Kornet L and Hoeks A P 2001 Assessment of the spatial homogeneity of artery dimension parameters with high frame rate 2-D B-mode *Ultrasound Med. Biol.* **27** 785–94

[17] Vappou J, Luo J and Konofagou E E 2010 Pulse wave imaging for noninvasive and quantitative measurement of arterial stiffness *in vivo Am. J. Hypertens.* **23** 393–8

[18] Feng J and Khir A W 2010 Determination of wave speed and wave separation in the arteries using diameter and velocity *J. Biomech.* **43** 455–62

[19] Khir A W, O'Brien A, Gibbs J S and Parker K H 2001 Determination of wave speed and wave separation in the arteries *J. Biomech.* **34** 1145–55

[20] Brands P J, Willigers J M, Ledoux L A, Reneman R S and Hoeks A P 1998 A noninvasive method to estimate pulse wave velocity in arteries locally by means of ultrasound *Ultrasound Med. Biol.* **24** 1325–35

[21] Cooper N P 1999 An improved heterodyne laser interferometer for use in studies of cochlear mechanics *J. Neurosci. Methods* **88** 93–102

[22] Willemin J-F F, Dändliker R and Khanna S M 1988 Heterodyne interferometer for submicroscopic vibration measurements in the inner ear *J. Acoust. Soc. Am.* **83** 787

[23] De Melis M, Morbiducci U, Scalise L, Tomasini E P, Delbeke D, Baets R, Van Bortel L M and Segers P 2008 A noncontact approach for the evaluation of large artery stiffness: a preliminary study *Am. J. Hypertens.* **21** 1280–3

[24] Brands P J, Hoeks A P, Ledoux L A and Reneman R S 1997 A radio frequency domain complex cross-correlation model to estimate blood flow velocity and tissue motion by means of ultrasound *Ultrasound Med. Biol.* **23** 911–20

[25] Chang C-W, Chen J-M, Wang W-K and Wang Y-Y L 2011 PWV measurement influenced by distance between two recording sites *Am. J. Hypertens.* **24** 250

[26] Hermeling E, Reesink K D, Kornmann L M, Reneman R S and Hoeks A P 2009 The dicrotic notch as alternative time-reference point to measure local pulse wave velocity in the carotid artery by means of ultrasonography *J. Hypertens.* **27** 2028–35

[27] Schulz U G and Rothwell P M 2001 Sex differences in carotid bifurcation anatomy and the distribution of atherosclerotic plaque *Stroke* **32** 1525–31

[28] Geinas J C *et al* 2012 Influence of posture on the regulation of cerebral perfusion *Aviat. Space Environ. Med.* **83** 751–7